ELSEVIER

Polymer 42 (2001) 3009–3021

polymer

www.elsevier.nl/locate/polymer

Order–disorder transition of polystyrene-*block*-polyisoprene Part II. Characteristic length as a function of polymer concentration, molecular weight, copolymer composition, and χ parameter

K. Mori[1], H. Hasegawa, T. Hashimoto*

Department of Polymer Chemistry, Graduate School of Engineering, Kyoto University, Yoshida-honmachi, Sakyo-ku, Kyoto 606-8501, Japan

Received 5 June 2000; received in revised form 2 September 2000; accepted 4 September 2000

Abstract

A series of polystyrene-*block*-polyisoprene diblock copolymers having various degrees of polymerization N_n and composition f_{PS} were studied as a function of temperature T and polymer concentration ϕ_p by means of in situ small-angle X-ray scattering methods. The results indicated that the characteristic length D as evaluated from $D = 2\pi/q_m$ with q_m being the wave number of the first-order scattering maximum was found to obey the following scaling law: $D \sim (\phi_p/T)^{1/3} N_n^{2/3}$ for $\phi_p/T \geq (\phi_p/T)_{MF} \sim N_n^{-1/2}$, and $D \sim (\phi_p/T)^0 N_n^{1/2}$ for $\phi_p/T \leq (\phi_p/T)_{MF}$ for the copolymer systems covered in this work. Here $(\phi_p/T)_{MF}$ is a crossover value of ϕ_p/T from the mean-field disordered state to the non-mean-field disordered state. These results are consistent with our previous experimental observations [Hashimoto et al., Macromolecules 16 (1983) 1093]. The results obtained here together with our previous results of $\chi_{eff} \sim (\phi_p/T) N_n^{-1/2}$ and $D_0 \sim N_n^{1/2}$ (Mori et al., J Chem Phys, 104 (1996) 7765) give the following scaling law:

$$D/D_0 \sim (\chi_{eff} N_n)^{1/3} \qquad \text{for } (\chi_{eff} N_n) \geq (\chi_{eff} N_n)_{MF}$$

and

$$D/D_0 \sim (\chi_{eff} N_n)^0 \qquad \text{for } (\chi_{eff} N_n) \leq (\chi_{eff} N_n)_{MF}$$

where χ_{eff} is an effective segmental interaction parameter between polystyrene and polyisoprene segments at a given ϕ_p and T for a given copolymer, and D_0 is the wavelength of the dominant mode of the concentration fluctuations of the copolymer systems in the mean-field disordered state. $(\chi_{eff} N_n)_{MF}$ is the crossover value of $\chi_{eff} N_n$ at the mean-field disordered state to the non-mean-field disordered state, which depends on f_{PS}.

Keywords: Block copolymers; Order–disorder transition; Polystyrene-*block*-polyisoprene

1. Introduction

In recent years, the phase transition of block copolymers has been extensively studied both theoretically and experimentally (see for example, the review articles in Refs. [1–4]). This phase transition has been elucidated to belong to the Brazovskii universality class where thermal agitation or thermal composition fluctuations play an important role [5]. These effects, called thermal fluctuation effects or Brazovskii effects, occur because the systems under consideration have a small characteristic length scale owing to a connectivity of the block chains in the block copolymers by a covalent bond in this case [1–3,6]. This *block connectivity* leads the phase transition of the systems to microphase transition or order–disorder transition (ODT) and to formation of microdomain structures having a characteristic length D on the order of radius of gyration R_g (~10 nm) of the block copolymers.

The thermal fluctuation effects were first suggested by Leibler [7] but were actually initiated to be explored theoretically by Fredrickson and Helfand [8], and experimentally by Bates et al. [9]. The effects have been shown to change the nature of the ODT for symmetric block copolymers from the second-order phase transition in the context

* Corresponding author. Tel.: +81-75-753-5604; fax: +81-75-753-4864.
E-mail address: hashimoto@alloy.polym.kyoto-u.ac.jp (T. Hashimoto).
[1] Present address: Film Research Center, Toyobo Company Ltd, Maehata, Kotsu, Inuyama, Aichi 484-8508, Japan.

0032-3861/01/$ - see front matter
PII: S0032-3861(00)00663-7

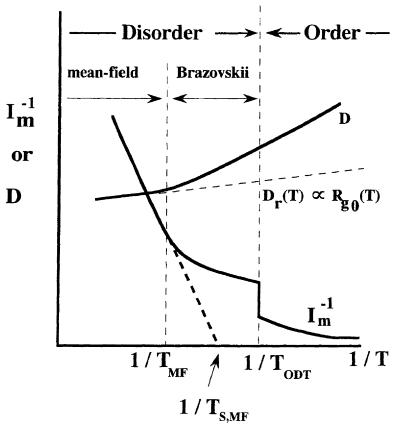

Fig. 1. Change in characteristic parameters I_m^{-1} and D with T^{-1} across the ODT temperature T_{ODT}. T_{MF} is the crossover temperature where the systems cross over from the mean-field disordered state to the non-mean-field disordered state.

of mean-field theory to the fluctuation-induced first-order phase transition [8,9]. The characteristics of this phase transition have been captured by scattering methods, such as small-angle X-ray scattering (SAXS) and small-angle neutron scattering (SANS) as schematically illustrated in Fig. 1 above [4,6,9–15].

Fig. 1 shows changes in D and I_m^{-1} with inverse absolute temperature T^{-1} across the ODT where $D = 2\pi/q_m$ where q_m is the scattering vector q at the maximum scattering intensity I_m [13]. Here the scattering vector is defined by $q = (4\pi/\lambda)\sin(\theta/2)$ where λ and θ are the wavelength of radiation and the scattering angle in a medium, respectively. At sufficiently high temperatures the systems are in the disordered states approximately characterized by the mean-field theory [7] so that I_m^{-1} linearly decreases with T^{-1} and temperature dependence of D is given by that of R_g. However, upon approaching ODT, the fluctuation effects become increasingly important so that changes in D and I_m^{-1} with T^{-1} start to deviate significantly from the mean-field behaviors described above: I_m^{-1} vs. T^{-1} plot is curved upward and temperature coefficient of D with T increases [13]. We "operationally" defined T_{MF} as a crossover temperature from the mean-field disordered state to the non-mean-field disordered state [13]. As temperature is further lowered, I_m^{-1} discontinuously decreases at a certain temperature, but the temperature dependence of D is unchanged. This temperature is identified to be the ODT temperature.

Before this concept of the thermal-fluctuation-induced first-order phase transition was established, we had conducted a series of studies on ODT [16–18]. In these studies, we overlooked the discontinuity of I_m^{-1} at ODT temperature and erroneously assigned T_{MF} in Fig. 1 to ODT temperature (T_c) as clearly stated on p. 7771 in Ref. [18] (part I of this series). Nevertheless, the previously reported scaling law [16,17] for the characteristic length D with the volume fraction ϕ_p, for absolute temperature T, and number-average degree of polymerization N_n of the particular block copolymers (two lamella-forming block copolymers coded as L-8 and L-2) in neutral solvents, as a whole is still valid [16,17], if $(\phi_p/T)_c$ for ODT is read as $(\phi_p/T)_{MF}$, the crossover point of the mean-field to non-mean-field disordered state [13]. However, the true ODT point $(\phi_p/T)_c$ is still left unevaluated in the series of our studies [16–18]. It has to be carefully determined by finding the discontinuity in I_m^{-1} with T^{-1}. In order to find the discontinuity, we should conduct scattering experiments across the ODT temperature with a small temperature increment.

The scaling law on $D(\phi_p/T; N_n)$ found by our experiment [16,17] is based upon the following two assumptions: the Flory effective segmental interaction χ_{eff} between PS and PI blocks in solutions is given by the *dilution approximation* [20,21],

$$\chi_{eff} = \chi_0 \phi_p \tag{1}$$

where χ_0 is the interaction parameter in melt (i.e. the case of $\phi_p = 1$) and χ_0 has a temperature dependence given by,

$$\chi_0 \sim 1/T \tag{2}$$

Eqs. (1) and (2) give

$$\chi_{eff} \sim \phi_p/T. \tag{3}$$

We conducted a series of work in order to check further the scaling law on D and the basic assumptions given by Eqs. (1) and (2). In part I of this series [18], we determined χ_{eff} as a function of T for the nine polystyrene-*block*-polyisoprene (SI) block copolymers having different N_n and fraction of the PS block, f_{PS}, by analyzing SAXS from the disordered copolymer solutions at $T > T_{MF}$ based upon Leibler's mean-field theory [7]. The results confirmed the validity of Eq. (3) over the temperature range covered in our experiment. Moreover, a series of SI with a given f_{PS} but different N_n yielded further information regarding N_n-dependence of χ_{eff},

$$\chi_{eff} \sim (\phi_p/T)N_n^{-1/2} \tag{4}$$

with proportionality being approximately a quadratic function of f_{PS} with a minimum at $f_{PS} \cong 1/2$ [18]. The dependence of χ_{eff} on N_n arises from that of χ_0 on N_n.

Since in the previous paper (part I of this series) we left the detailed analyses of the scaling law on D as a function of ϕ_p/T, N_n, and f_{PS} unexplored, in this paper (part II of this series) we will study it for the same series of SI to check applicability of the scaling laws [16,17] previously found only for the two SI block copolymers. Moreover, by using the scaling law found in part I on χ_{eff} (Eq. (4)), we shall advance our argument a step further to obtain a relationship between D and the segregation power $\chi_{eff}N_n$ of the block copolymer solutions. Our analysis is based on the assumption that χ_{eff} evaluated in the mean-field disordered state can be extended to the non-mean-field disordered state and ordered state by extrapolating the

Table 1
Characteristics of SI copolymers used in this experiment

Sample code	$M_n \times 10^3$	PS (wt%)	M_w/M_n	N_n	f_{PS}	Polymerization solvent	Ref.[a]
HK-17	6.8	50	1.2	80.6	0.468	THF	[19]
HK-15	17.4	55	1.2	206	0.518	THF	[18]
L-2	31	40		374	0.369	THF	[16,17]
TSI-3	32	59	1.12	377	0.555	Benzene	[20]
HS-12	75.4	46	1.05	900	0.425	Benzene	
L-8	94	50		1120	0.464	Benzene	[16,17]
HS-16	22	74	1.02	254	0.715	THF	[18]
TSI-2	30	77	1.14	344	0.744	Benzene	[18]
HS-15	42	76	1.02	486	0.736	THF	[18]
HS-7	51	31	1.04	621	0.283	THF	[18]
TOKI-4	94	20	1.07	1168	0.178	Benzene	

[a] References where the SAXS profiles were presented.

relation of χ_{eff} vs. $1/T$ obtained in the mean-field disordered state to the respective states. The experimentally established scaling law will be compared with some theoretical predictions [22–24].

2. Experimental methods

The SI block copolymers used in this work are the same as those used in part I [18]. The dioctylphthalate (DOP) solutions of the copolymers with various concentrations were prepared also in the same way as in part I. DOP is a solvent neutral for PS and PI. SAXS measurements were conducted in situ as a function of T at given copolymer concentrations ϕ_p, in the same way as in part I. Table 1 summarizes the characteristics of the copolymers used in this work. In Table 1, N_n and f_{PS} were evaluated by taking asymmetry of the segmental volume into account after Helfand [19],

$$N_n \equiv (\rho_{0S}\rho_{0I})^{1/2}[(N_{PS}/\rho_{0S}) + (N_{PI}/\rho_{0I})] \quad (5)$$

and

$$f_{PS} \equiv (N_{PS}/\rho_{0S})/[(N_{PS}/\rho_{0S}) + (N_{PI}/\rho_{0I})] \quad (6)$$

Here the quantity ρ_{0S} is the segmental density of the PS block (1.01×10^4 mol/m^3), ρ_{0I} is that of the PI block (1.34×10^4 and 1.36×10^4 mol/m^3 for the PI block rich in 1,4- and 3,4-linkages, respectively), and N_{PS} and N_{PI} are the number-average degree of polymerization for the PS and PI blocks, respectively.

The eleven SI block copolymers in Table 1 can be classified into three groups: the one having $f_{PS} \cong 0.5$ so that their ordered structure is lamellar microdomains (from HK-17 to L-8 in Table 1), the one having $f_{PS} \cong 0.75$ or 0.3 (from HS-16 to HS-7) and the one having $f_{PS} \cong 0.2$ (TOKI-4), the latter two groups showing cylindrical microdomains in the ordered state. The copolymers prepared in benzene and tetrahydrofuran (THF) have the microstructure of PI rich in 1,4- and 3,4-linkages, respectively, and hence their statistical segment lengths are 0.63 and 0.59 nm, respectively [25]. The different microstructure of the PI block would give different χ_{eff} against the PS block, as will be discussed later.

3. Results

Typical SAXS profiles for the SI copolymers having $f_{PS} \cong 0.5$ were previously presented as a function of ϕ_p, T and N_n for L-2 and L-8 [16,17], HK-15 [18], HK-17 [26], and TSI-3 [20]. The way in which the SAXS profiles for these SI copolymers having $f_{PS} \cong 0.5$ depend on ϕ_p, T and N_n is similar to the cases of L-2 and L-8. Therefore, we show here only the SAXS profiles of TSI-2 and HS-15 as a function of ϕ_p and T as typical examples of the SI copolymers having $f_{PS} \cong 0.75$, since a part of the profiles for HS-16 and HS-7 as well were already shown previously at particular ϕ_p and T [18].

Fig. 2 shows the temperature dependence of the SAXS profiles for HS-15 at various concentrations. The profiles for the bulk specimen (part a) are typical to those for the hexagonally packed cylindrical microdomains, showing maxima or shoulders at the scattering vectors corresponding to $1 : \sqrt{3} : \sqrt{4} : \sqrt{7} : \sqrt{9}$, etc. relative to the q value of the first-order scattering maximum. As temperature is raised, the maxima or shoulders become increasingly broader and shift toward higher q values and their peak intensities decrease. Note that each profile at a higher temperature is shifted vertically by one decade relative to that at a lower temperature, in order to avoid an overlap of the profiles at various temperatures. The same vertical shift was applied also for the other concentrations and for other block copolymer solutions.

The profiles for the 80% DOP solution (part b) show a temperature dependence similar to that for bulk. The peak shift toward larger scattering vector q with increasing T is

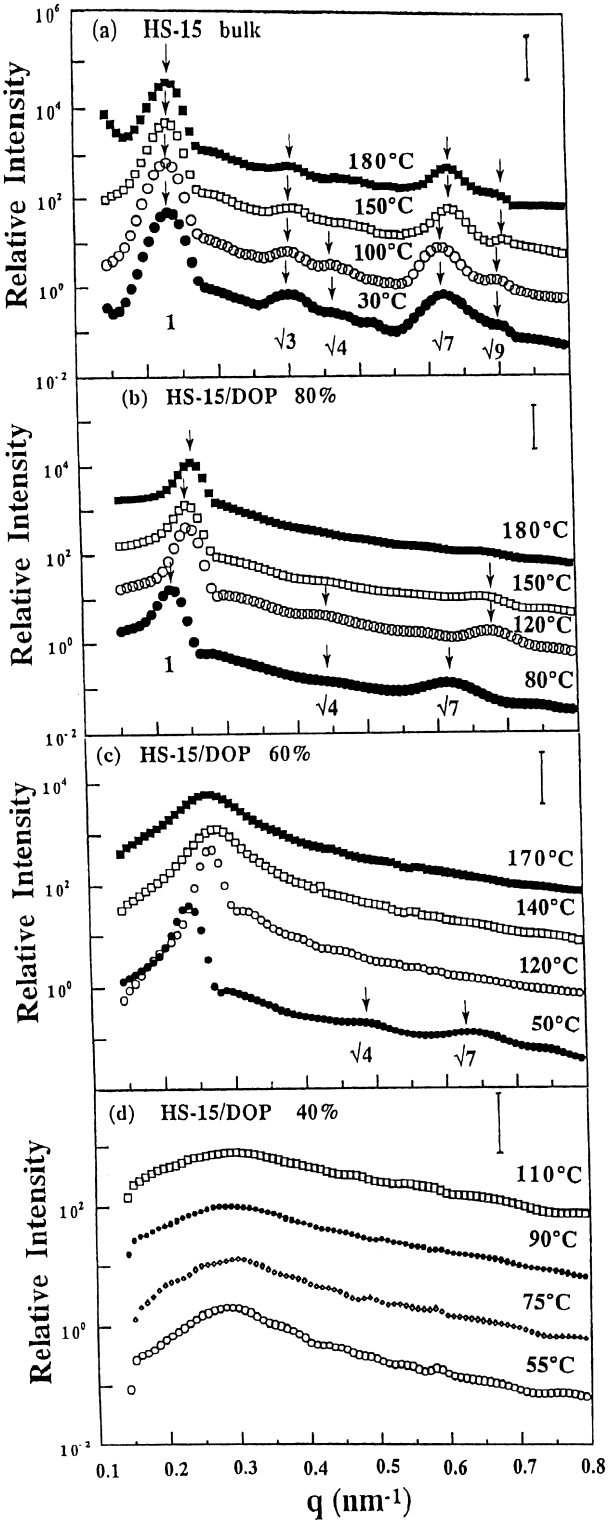

Fig. 2. SAXS profiles for HS-15 in: (a) bulk, (b) 80, (c) 60 and (d) 40% DOP solutions at various temperatures. The bar indicates the amount of the vertical shift between the successive profiles to avoid their overlaps.

more clearly seen, especially for the first-order peak. The broadening and intensity decrease of the higher-order peaks or shoulders are also very remarkable. A drastic change of the profiles with T is seen for the 60% DOP solution (part c): upon increasing T up to 120°C, the first-order peak broadens and shifts toward the higher q value, and the higher-order peaks decrease their intensity and disappear, resulting in only the first-order peak being clearly discerned. Upon further increase of T above 140°C, only the first-order peak is discerned. The first-order peak broadens very much, but its position hardly changes with T. There is a dramatic change of the profile with T between 120 and 140°C.

For the lowest copolymer concentration (the 40% DOP solution shown in part d), the SAXS profiles show only the very broad first-order peaks whose positions q_m are essentially independent of T. The positions q_m are equal to those for the 60% copolymer solutions at $T \geq 140$°C. Thus, the broad first-order peaks have their positions essentially independent of ϕ_p and T. We will show later that these broad first-order peaks are due to the concentration fluctuations of the PS and PI segments of the copolymers in the disordered state and the position q_m is related to the wavelength D of the dominant mode of the concentration fluctuations. On the other hand, the peak position q_m at lower temperatures and higher concentrations shifts with T and ϕ_p, reflecting T- and ϕ_p-dependence of the Bragg spacing D for the cylindrical microdomains (see parts a and b at all T, and part c at $T \leq 120$°C). Obviously, D decreases with increasing T and decreasing ϕ_p.

Fig. 3 shows the temperature dependence of the SAXS profiles for TSI-2 at various concentrations. TSI-2 has the composition f_{PS} similar to that for HS-15 but has N_n lower than that for HS-15. TSI-2 for the bulk (part a) shows the first- and higher-order scattering maxima or shoulders at scattering vectors of $1 : \sqrt{3} : \sqrt{7}$ relative to the q value of the first-order maximum at $T \leq 170$ and $T \leq 60$°C for the 80% DOP solution, indicating that the hexagonally packed cylindrical microdomains exist in these melts and solutions. In these concentration and temperature ranges, the scattering profiles show the same T- and ϕ_p-dependence as that for HS-15 in the ordered state. The maximum scattered intensity decreases, and the scattering peaks become broader and shift toward larger q values with increasing T and decreasing ϕ_p, indicating that both amplitude and the characteristic length of the concentration fluctuations decrease with increasing T and decreasing ϕ_p.

At $T \geq 210$°C for the bulk (part a), $T \geq 105$°C for the 80% solution (part b) and at all T for the 60% solution, the SAXS profiles show only a single broad peak whose intensity decreases with increasing T and decreasing ϕ_p but whose position is essentially independent of ϕ_p and T. The broad peaks reflect again D being independent of T and ϕ_p, as will be shown later.

TSI-2 has the SAXS maxima or shoulders at the scattering angles higher than those for HS-15, indicating that it has D smaller than those for HS-15. A close comparison of Figs. 2 and 3 also reveals that TSI-2 becomes the disordered state at lower T and higher ϕ_p than HS-15. These two observations clearly reflect the effects of molecular weight on concentration fluctuations as will be discussed in detail later.

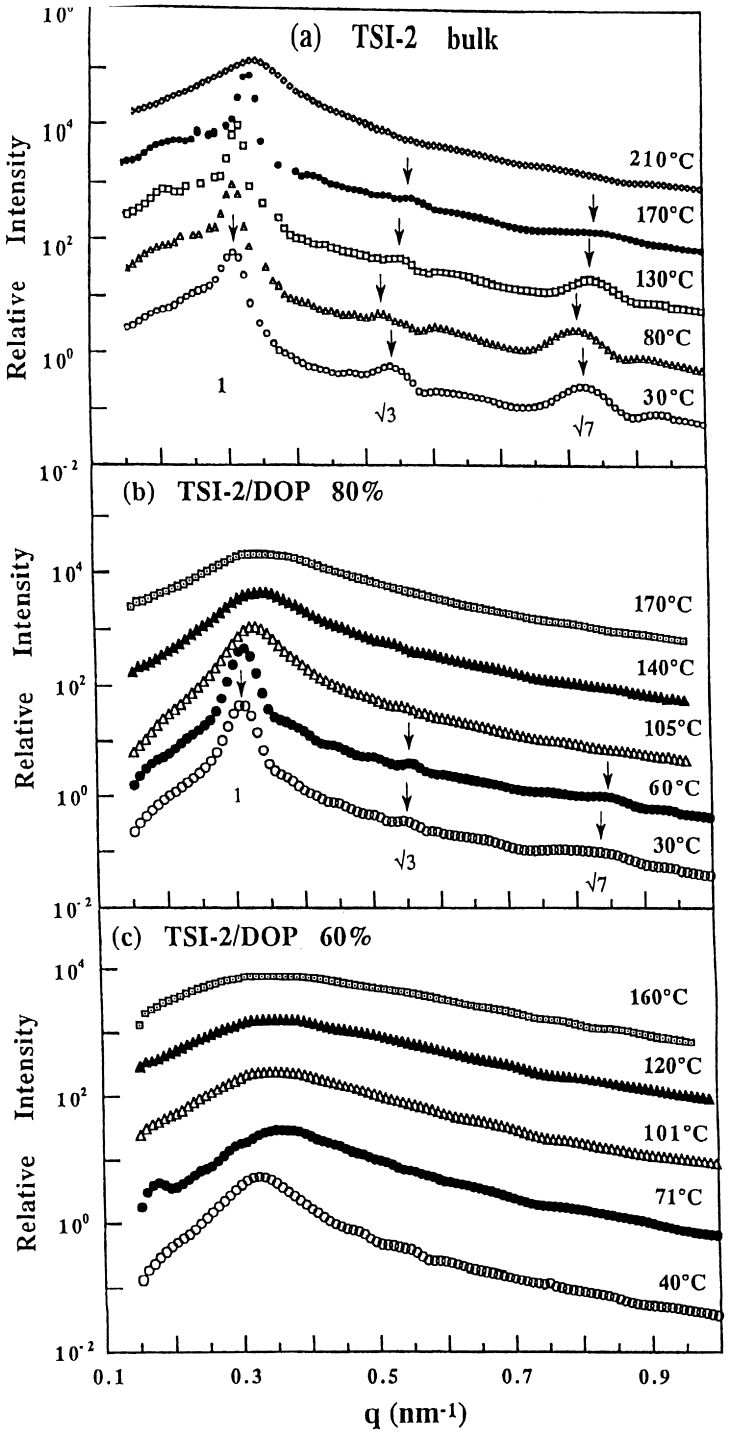

Fig. 3. SAXS profiles for TSI-2 in: (a) bulk, (b) 80 and (c) 60% DOP solutions at various temperatures.

4. Analysis and discussion

4.1. Conventional analysis

In this section we follow the same analysis as we previously employed for L-2 and L-8 [16,17], but we extend this analysis for a wide variety of the copolymers having different N_n and f_{PS}.

4.1.1. D as a function of ϕ_p/T

Since the wavelength D of the dominant mode of the concentration fluctuations depends on χ_{eff}, and χ_{eff} for a

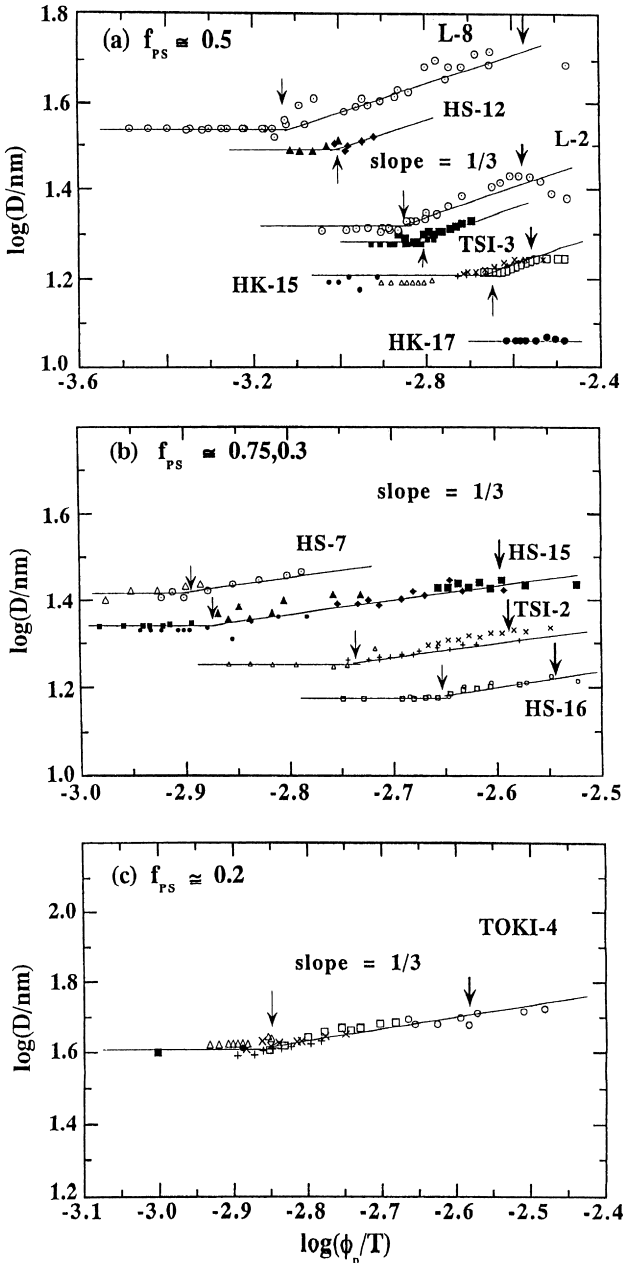

Fig. 4. Temperature (T) and concentration (ϕ_p) dependence of the wavelength D of the dominant mode of the concentration fluctuations for the various SI copolymers having $f_{PS} \cong 0.5$ (a), 0.75 or 0.3 (b), and 0.2 (c). The thin arrows indicate the crossover points $(\phi_p/T)_{MF}$ from the mean-field to non-mean-field disordered state and the thick arrows indicate the points $(\phi_p/T)_f$ above which the non-equilibrium effect becomes significant.

given copolymer with a fixed value of N_n and that of f_{PS} depends on ϕ_p/T (Eq. (3) or Eq. (4)), we plotted D obtained at various T and ϕ_p against ϕ_p/T in the double logarithmic scale. The results are shown in Fig. 4 where parts a–c were obtained for the copolymers having $f_{PS} \cong 0.5$, 0.75 or 0.3, and 0.2, respectively.

For the copolymers having $f_{PS} \cong 0.5$, there is the regime satisfying $\phi_p/T \leq (\phi_p/T)_{MF}$ where D is independent of ϕ_p/T and the regime $\phi_p/T \geq (\phi_p/T)_{MF}$ where D tends to increase with the 1/3-power law, as found previously for L-2 and L-8 [16,17], the data of which were included in Fig. 8a for comparison i.e.

$$D \sim (\phi_p/T)^0 \qquad \text{for } (\phi_p/T) \leq (\phi_p/T)_{MF} \tag{7}$$

$$D \sim (\phi_p/T)^{1/3} \qquad \text{for } (\phi_p/T) \geq (\phi_p/T)_{MF} \tag{8}$$

$(\phi_p/T)_{MF}$ designates the crossover point (concentration at a given temperature or temperature at a given concentration) from the mean-field disordered state to the non-mean-field disordered state as described earlier. The small temperature dependence of D in the mean-field disordered state as depicted in Fig. 1 cannot be discerned in the ordinate scale used for Fig. 4.

D at a given (ϕ_p/T) depends on N_n: the greater the value of N_n, the larger the D value. The crossover point $(\phi_p/T)_{MF}$ also depends on N_n; the greater the value of N_n, the smaller the value of $(\phi_p/T)_{MF}$ as shown by thin arrows. All these trends are consistent with those previously found with L-2 and L-8.

The downward deviations of the data point from the straight lines at the value of ϕ_p/T greater than $\log(\phi_p/T)_f \cong -2.6$ (shown by thick arrows) are due to the non-equilibrium effects caused primarily by vitrification of the systems [16,17,27]. HK-17 is vitrified in the disordered state before it reaches the order–disorder transition point [26]. Owing to the fact that the vitrification occurs at nearly constant $(\phi_p/T)_f$, the change of D with (ϕ_p/T) is smaller for the copolymers having smaller N_n than for those having larger N_n (cf. L-8 and L-2 in part a, HS-15 and HS-16 in part b). Since the vitrification process is beyond the scope of the present work, we shall hereafter (e.g. in Figs. 7 and 8, later) exclude the data on D that belong to this vitrification regime from the data in the thermal equilibrium regime $[(\phi_p/T) < (\phi_p/T)_f]$.

Essentially the same trends as those found for the copolymers having $f_{PS} \cong 0.5$ are also found for the copolymers having $f_{PS} \cong 0.75$, 0.3 (part b) and 0.2 (part c). Thus the empirical scaling laws of Eqs. (7) and (8) found with only two block copolymers L-2 and L-8 [16,17] having the lamellar domains in the ordered state are qualitatively confirmed for many copolymer systems used in this work, including also the systems having the cylindrical domains in the ordered state. The proportionality constant of Eqs. (7) and (8) depends generally on N_n and f_{PS}. The crossover point $(\phi_p/T)_{MF}$ also depends on N_n and f_{PS}, which will be shown more clearly in Fig. 6 later.

It should be noted that the behavior of D as a function of ϕ_p/T depends not only on N_n and f_{PS} but also on the microstructure of the PI block, causing a horizontal shift in the plots of $\log D$ vs. $\log(\phi_p/T)$, because χ_0 depends on the microstructure. However, we shall not concern ourselves with this microstructure effect here, simply because the microstructure effect will disappear when D is scaled with χ_{eff} as will be detailed in Section 4.2.

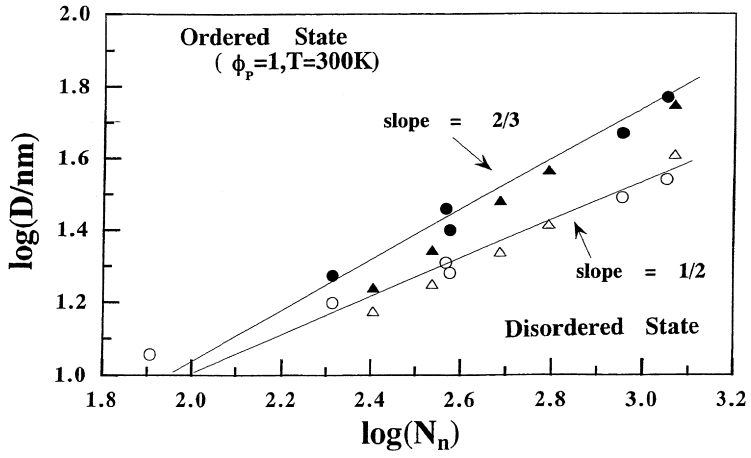

Fig. 5. Wavelength D of the dominant mode of the concentration fluctuations in the ordered state at $\phi_p = 1$ and $T = 300$ K (filled circles and triangles) and in the disordered state (independent of ϕ_p and T, open circles and triangles) plotted as a function of N_n in double logarithmic scales. The circles refer to the data for SI having $f_{PS} \cong 0.5$ and the triangles to the data for SI having $f_{PS} \cong 0.75$, 0.3 and 0.2.

4.1.2. D as a function of N_n

Fig. 5 shows the D spacing for the ordered state (D_{order}) (filled symbols) at $(\phi_p/T) = 1/300\ K^{-1} \gg (\phi_p/T)_{MF}$ and that for the mean-field disordered state ($D_{disorder}$) (open symbols), as a function of N_n in double logarithmic scales. To estimate the D value in the ordered state, we extrapolated the straight lines in the plot of log D vs. $\log(\phi_p/T)$ with slope 1/3 in Fig. 4 and read the D values at $\phi_p/T = 1/300\ K^{-1}$ [$\log(\phi_p/T) = -2.48$]. Table 2 summarizes D_{order} at this (ϕ_p/T) and $D_{disorder}$ as well. The spacing D_{order} for the copolymers having $f_{PS} \cong 0.5$ were shown by filled circles, while those for $f_{PS} \cong 0.75$ and 0.2–0.3 were shown by filled triangles. The spacings are not a strong function of f_{PS} for the copolymers covered in this work and approximately fall on the same straight line with the slope of 2/3 as shown in Fig. 5,

$$D_{order} \sim N_n^{2/3}, \tag{9}$$

thus confirming the 2/3-power [28–30], i.e. the implication of the behavior in the so-called strong segregation regime, which will be further discussed later in Section 4.2. This result together with Eq. (8) gives

$$D_{order} \sim (\phi_p/T)^{1/3} N_n^{2/3}, \tag{10}$$

hence confirming the scaling law previously reported for L-2 and L-8 [16,17].

The spacings in the mean-field disordered state are shown by open circles for the copolymers with $f_{PS} \cong 0.5$ and by open triangles for the other copolymers. Note that the spacings in the disordered state are independent of ϕ_p and T, as shown in Fig. 4. Again, the spacings approximately fall on the same straight line with the slope 1/2 for the range of f_{PS} covered in this work, confirming the previous finding [16,17],

$$D_{disorder} \sim N_n^{1/2}, \tag{11}$$

This result and Eq. (7) give

$$D_{disorder} \sim (\phi_p/T)^0 N_n^{1/2}, \tag{12}$$

with the proportionality constant generally dependent upon f_{PS}.

4.1.3. Crossover point $(\phi_p/T)_{MF}$ as a function of N_n and f_{PS}

The crossover points $(\phi_p/T)_{MF}$ as characterized by the inflection points in the plots of log D vs. $\log(\phi_p/T)$ in Fig. 4 are plotted against N_n in the double logarithmic scales in Fig. 6. The values $(\phi_p/T)_{MF}$ for the copolymers at given f_{PS} tend to decrease with increasing N_n, which is approximately given by

$$(\phi_p/T)_{MF} \sim N_n^{-1/2} \tag{13}$$

This result again confirms our previous result [16,17]. The proportionality constant is found to depend significantly on f_{PS}: the ODT occurs at the lowest concentration and highest temperature for the copolymers having $f_{PS} \cong 0.5$ among the

Table 2
D_{order} and $D_{disorder}$ estimated from Fig. 4

Sample code	f_{PS}	N_n	D_{order} (nm)[a]	$D_{disorder}$ (nm)[b]
HK-17	0.468	80.6		11.4
HK-15	0.518	206	18.8	15.8
L-2	0.369	374	28.8	20.4
TSI-3	0.555	377	25.1	19.1
HS-12	0.425	900	46.7	30.9
L-8	0.464	1120	58.9	34.7
HS-16	0.715	254	17.4	15.0
TSI-2	0.744	344	22.1	17.8
HS-15	0.736	486	30.3	21.8
HS-7	0.283	621	36.9	26.0
TOKI-4	0.178	1168	56.2	40.7

[a] The D values estimated at $\phi_p/T = 1/300\ K^{-1}$ using Fig. 4.
[b] The D values at the mean-field disordered state, $\phi_p/T < (\phi_p/T)_{MF}$.

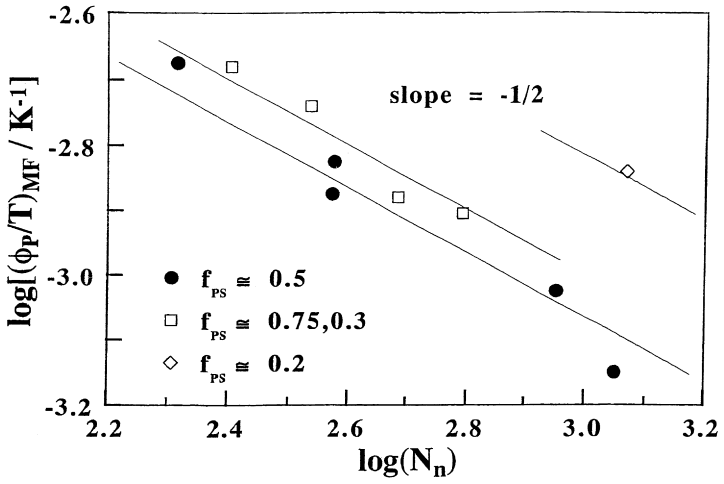

Fig. 6. Crossover points $(\phi_p/T)_{MF}$ plotted as a function of N_n in double logarithmic scales for the various SI copolymers with $f_{PS} \cong 0.5$, 0.75 or 0.3, and 0.2.

Table 3
Summary of the crossover temperatures T_{MF} for various SI copolymers at various concentrations ϕ_p

Sample code	f_{PS}	N_n	ϕ_p	T_{MF}	Remarks[a]
HK-17	0.468	80.6	1	–	1
HK-15	0.518	206	1	160	2
			0.89	140	2
			0.81	110	2
			0.49	–	1
			0.37	–	1
L-2	0.369	374	1	–	3
			0.57	190	2
			0.473	90	2
			0.374	–	1
			0.27	–	1
TSI-3	0.555	377	0.6	123	2
			0.5	49	2
HS-12	0.425	900	0.365	69	2
			0.302	60	2
L-8	0.464	1120	1	–	3
			0.67	–	3
			0.43	–	3
			0.25	90	2
			0.2	–	1
			0.15	–	1
HS-16	0.715	254	1	171	2
			0.8	111	2
TSI-2	0.744	344	1	–	3
			0.8	131	2
			0.6	100	2
HS-15	0.736	486	1	–	3
			0.8	–	3
			0.6	–	3
			0.5	123	2
			0.4	–	1
HS-7	0.283	621	0.494	111	2
			0.395	69	2
TOKI-4	0.178	1168	1	–	3
			0.63	–	3
			0.54	–	3
			0.424	49	2

[a] Numbers 1–3 designate, respectively, (1) mean-field (MF) disordered state at all temperatures, (2) MF disordered state at $T > T_{MF}$, and (3) ordered state at all temperatures.

copolymers covered in our work. For the copolymer with $f_{PS} = 0.2$, we just assumed the same N_n-dependence as those found for the copolymers with $f_{PS} \cong 0.5$, 0.75 and 0.3. Table 3 summarizes the crossover temperature T_{MF} measured as a function of ϕ_p for each copolymer studied in this work.

4.2. D as a function of χ_{eff}

Since in our previous work [18] we determined χ_{eff} as function of ϕ_p and T for each copolymer used in this work, we use the data on χ_{eff} for analyzing D as a function of χ_{eff}. To do this, we extrapolate the χ_{eff} values obtained in the mean-field disordered state to the temperature below T_{MF} by using Eq. (14) shown below. In our previous work [18], χ_{eff} in Eq. (1) was shown to be given by

$$\chi_{eff} = \phi_p(A + B/T) \tag{14}$$

with A and B generally depending on f_{PS} and N_n. Table 4 lists the values of A and B previously estimated for each copolymer [18] along with the crossover values $(\phi_p/T)_{MF}$, $\chi_{eff,MF}$ and $(\chi_{eff}N_n)_{MF}$. Here $(\phi_p/T)_{MF}$ were estimated in the previous section, while $\chi_{eff,MF}$ and $(\chi_{eff}N_n)_{MF}$ will be estimated from the plot shown in Fig. 7.

Fig. 7 shows double logarithmically D as a function of χ_{eff} for the copolymers having $f_{PS} \cong 0.5$ (part a), 0.75 or 0.3 (part b) and 0.2 (part c). The results shown in Fig. 7 were obtained from the results in Fig. 4 along with the values of A and B in Table 4 and Eq. (14). The results tend to show

$$D \sim \chi_{eff}^{1/3} \qquad \text{for } \chi_{eff} \geq \chi_{eff,MF} \tag{15}$$

$$D \sim \chi_{eff}^{0} \qquad \text{for } \chi_{eff} \leq \chi_{eff,MF} \tag{16}$$

within experimental accuracy. It should be noted that the data for L-8 and L-2 were not included in Fig. 7a, simply because the data for χ_{eff} were not measured for these copolymers [16–18]. The values of D as a function of N_n are given by Eqs. (9) and (11), respectively. The inflection

Table 4
Coefficients A and B, which determine temperature dependence of χ_{eff}, and crossover points $\chi_{eff,MF}$, $(\chi_{eff}N_n)_{MF}$, and $(\phi_p/T)_{MF}$ (K^{-1}) for various SI copolymers

Sample code	f_{PS}	N_n	A[a]	B[a]	$\chi_{eff,MF}$	$(\chi_{eff}N_n)_{MF}$	$(\phi_p/T)_{MF}\times 10^3$ (K^{-1})
HK-17	0.468	80.6	−0.0759	63.9			
HK-15	0.518	206	−0.0297	33.5	0.0501	10.324	2.11
L-2	0.369	374	−0.00984[b]	19.86[b]	0.0176	6.69	1.38
TSI-3	0.555	377	−0.00133	16.07	0.0237	8.94	1.5
HS-12	0.425	900	−0.00183	12.07	0.0110	9.914	0.944
L-8	0.464	1120	0.00227[b]	9.51[b]	0.0093	10.46	0.741
HS-16	0.715	254	−0.0386	42.2	0.0580	14.9	2.138
TSI-2	0.744	344	−0.032	38.23	0.0493	16.96	1.82
HS-15	0.736	486	−0.012	29.6	0.0320	15.54	1.244
HS-7	0.283	621	−0.0116	23.2	0.0229	14.26	1.244
TOKI-4	0.178	1168	−0.006	20.21	0.0251	29.34	1.445

[a] The coefficients which determine temperature dependence of χ_{eff} (see Eq. (14)).
[b] The value estimated from Figs. 10 and 11 in Ref. [18].

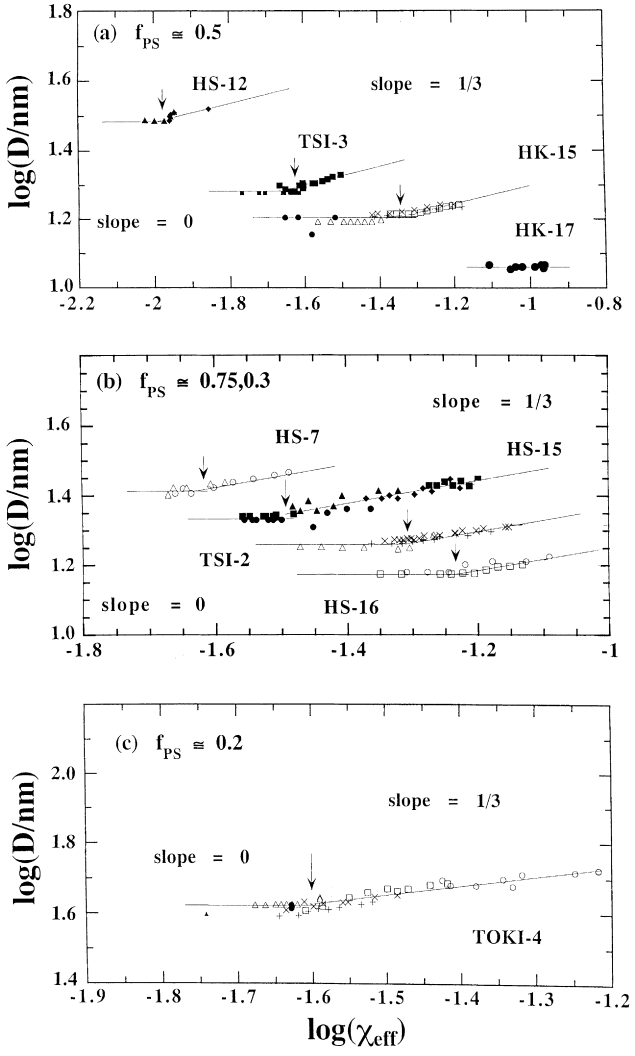

Fig. 7. Wavelength D of the dominant mode of the concentration fluctuations plotted as a function of χ_{eff} in double logarithmic scales for the various copolymers having $f_{PS} \cong 0.5$ (a), 0.75 or 0.3 (b), and 0.2 (c). The thin arrows have the same meaning as those in Fig. 4.

points $\chi_{eff,MF}$ shown by thin arrows give the crossover points, which are summarized in Table 4. $\chi_{eff,MF}$ is a function of N_n and f_{PS} as seen in Fig. 7 and as will be clearly shown in Fig. 9 later.

4.3. D/D_0 as a function of $\chi_{eff}N_n$

The dependence of D and $\chi_{eff,MF}$ on N_n shown in Fig. 7 can be further rescaled, respectively, by taking a ratio of D/D_0 where $D_0 \equiv D_{disorder}$ and by taking a product of $\chi_{eff}N_n$. A test of this scaling law is shown in Fig. 8 in the double logarithmic scales for the copolymers with $f_{PS} \cong 0.5$ (part a), 0.75 or 0.3 (part b) and 0.2 (part c). Although the data points are scattered to some extent, the data obtained at various ϕ_p, T and N_n fall on a master curve reasonably well for the copolymers having nearly equal f_{PS} in the range of temperature and ϕ_p where the non-equilibrium effects do not come into a play, i.e. in the regime of relatively low values of $\chi_{eff}N_n$. The results indicate that: (i)

$$(\chi_{eff}N_n)_{MF} = \text{constant} \tag{17}$$

with the dimensionless constant depending only on f_{PS}, the reduced crossover point are shown by thin arrows in Fig. 8, and (ii) D/D_0 is given by

$$D/D_0 \sim (\chi_{eff}N_n)^0 \qquad \text{for } \chi_{eff}N_n \leq (\chi_{eff}N_n)_{MF} \tag{18}$$

and

$$D/D_0 \sim (\chi_{eff}N_n)^{1/3} \qquad \text{for } \chi_{eff}N_n \geq (\chi_{eff}N_n)_{MF} \tag{19}$$

Eq. (17) is consistent with the mean-field theory [7] within our experimental accuracy. Although Eq. (17) does not directly indicate the mean-field critical point, there may be a parallelism between the crossover point and the mean-field critical point. *Eq. (19) is obtained from a combination of the two experimental results: one giving rise to Eq. (10) and the other giving rise to the unique molecular weight dependence of χ_{eff} as given by Eq. (4).* The relation $D \sim N_n^{2/3}$ in Eq. (10) apparently implies that the systems are in the strong segregation limit [28–30]. However, if χ_{eff}

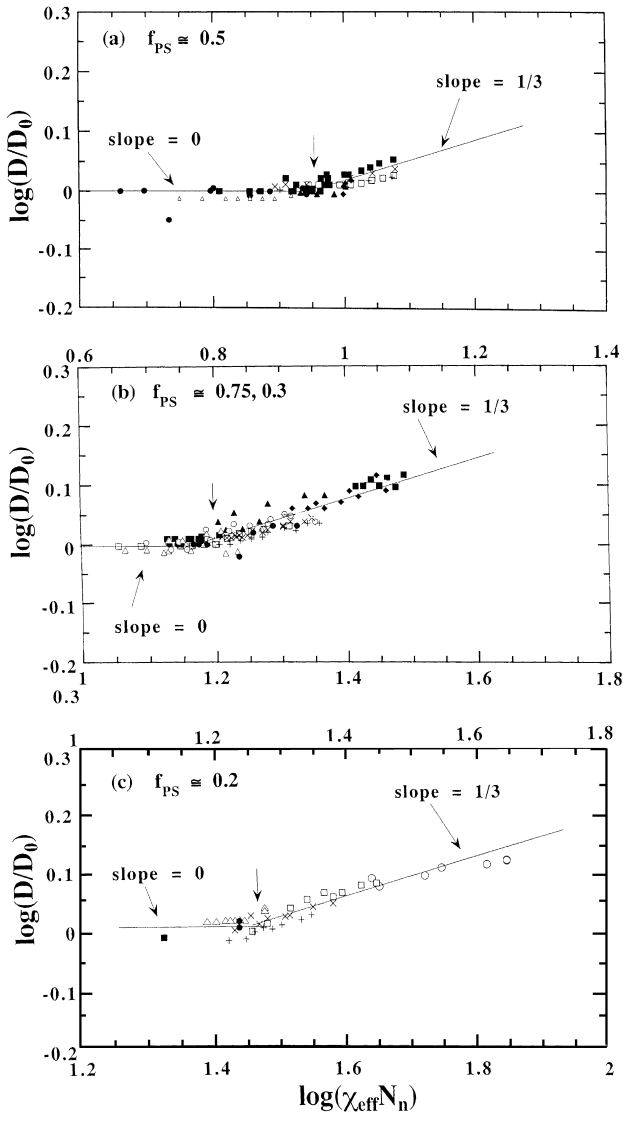

Fig. 8. Reduced wavelength D/D_0 plotted against the segregation power $\chi_{eff}N_n$ in double logarithmic scales for the various SI copolymers having $f_{PS} \cong 0.5$ (a), 0.75 or 0.3 (b), and 0.2 (c). The value D and the thin arrows have the same meanings as those in Fig. 4. The value D_0 designates the value D in the mean-field disordered state. The data subjected from the non-equilibrium effects are omitted from these plots.

depends on N_n and a part of exponent 2/3 comes from the N_n-dependence of χ_{eff}, we obtain Eq. (19) for the quantity D/D_0 as a function of the effective segregation power $\chi_{eff}N_n$ of the systems. The exponent 1/3 is not the one typical to the *strong segregation limit*, for which the exponent should be 1/6, but rather is typical to the *intermediate segregation regime* [22–24] as will be discussed later. Thus, to our big surprise, the N_n-dependence of χ_{eff} alters our interpretation of the exponent 2/3 in the 2/3-power law ($D \sim N_n^{2/3}$).

4.4. Crossover point from mean-field to non-mean-field disordered state

Fig. 9 shows the crossover value of χ_{eff} as obtained from Fig. 7 and summarized in Table 4 as a function of N_n. The results confirm Eq. (17) with the constant depending upon f_{PS} as shown in Fig. 10. The results given in Figs. 9 and 10 are apparently consistent with Leibler's prediction on the mean-field ODT point within our experimental accuracy, implying a qualitative parallelism between the crossover point and the mean-field ODT point. However, it should be noted that this finding was obtained only after renormalizing the ϕ_p and N_n-dependence of χ_{eff} as given by Eq. (4).

4.5. Comparisons with previous experimental results

The data on L-8 and L-2 are not included in Fig. 8a, simply because the data on χ_{eff} were not available for these systems. However, if we apply the relationships between A vs. N_n, B vs. N_n, and $BN_n^{0.7}$ vs. f_{PS}, which were obtained in the previous paper (see Figs. 10 and 11 of Ref. [18]), to L-8 and L-2, we can evaluate the values of χ_{eff} for these systems as well. These values thus estimated are also listed in Table 4. The results on $\log(D/D_0)$ vs. $\log(\chi_{eff}N_n)$ thus obtained for L-8 and L-2 are shown in Fig. 11a, revealing that the scaling law given by Eqs. (18) and (19) are legitimate for these systems as well. The results in Fig. 11a are compared with those obtained in Fig. 8a for the series of SI with $f_{PS} \cong 0.5$ in Fig. 11b (see the data shown by open symbols).

Similarly, a series of data for the SI block copolymers in

Table 5
Coefficients A and B, which determine temperature dependence of χ_{eff}, and crossover points $\chi_{eff,MF}$, $(\chi_{eff}N_n)_{MF}$ and $(\phi_p/T)_{MF}$ for L-1 to L-8 specimens previously studied [29]

Sample code	f_{PS}	N_n	A[a]	B[a]	$\chi_{eff,MF}$[b]	$(\chi_{eff}N_n)_{MF}$[b]	$(\phi_p/T)_{MF} \times 10^3$ (K^{-1})[b]
L-1	0.491	253	−0.0189	26.98	0.0398	10.07	2.176
L-2	0.363	381	−0.00984	19.86	0.026	9.906	1.805
L-3	0.411	598	−0.00378	14.82	0.0167	9.987	1.382
L-4	0.421	670	−0.00151	13.65	0.0148	9.936	1.197
L-5	0.471	1172	0.00227	9.25	0.0084	9.786	0.657
L-6	0.572	1213	0.00227	9.00	0.008	9.74	0.64
L-8	0.464	1120	0.00227	9.51	0.0093	9.912	0.741

[a] The values estimated from Figs. 10 and 11 in Ref. [18].
[b] The values estimated from Fig. 9.

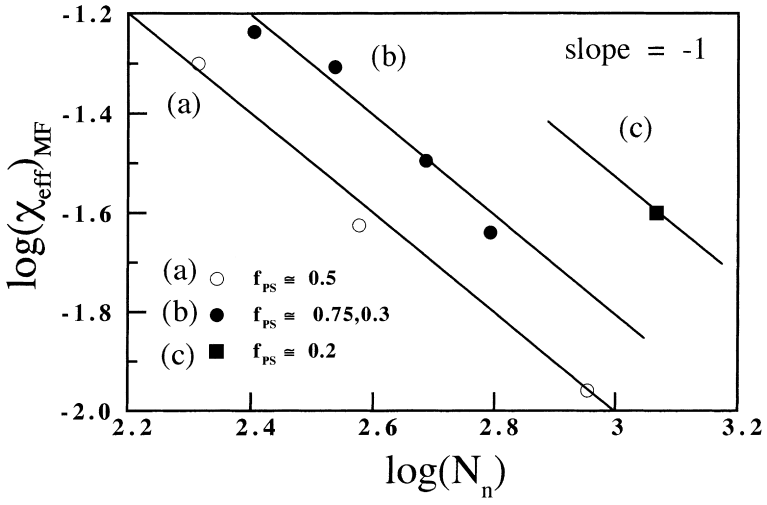

Fig. 9. χ_{eff} at the crossover point $(\chi_{eff})_{MF}$ plotted against N_n in double logarithmic scales for the SI copolymers having $f_{PS} \cong 0.5$ (a), 0.75 or 0.3 (b), and 0.2 (c).

bulk [29] showing the 2/3-power law of $D \sim M_n^{2/3}$, which are thought to be typical to the data for the strong segregation limit, were applied to the same analysis as described above. The results are shown in Fig. 12. The parameters A and B estimated and used to obtain Fig. 12 are shown in Table 5 together with the parameters evaluated from Fig. 12. The figure includes the results obtained for a series of new SI diblocks showing the cylindrical morphology, characteristics of which are summarized in Table 6. The results are consistent with those found for the other systems discussed earlier. All these results may suggest that the systems we studied are not yet in the truly strong segregation limit.

4.6. Comparisons with some theoretical predictions

Quantitative comparisons between the experimental results and theoretical predictions are difficult because of difficulties in quantitative evaluation of the χ_{eff} values. Nevertheless, we attempt to qualitatively compare the experimental and theoretical trends.

Fig. 13 shows some representative theoretical results by Whitmore and Noolandi (WN) [22] and Lescanec and Muthukumar (LM) [23] for diblock copolymers with the volume fraction of one of the components f equal to 0.5

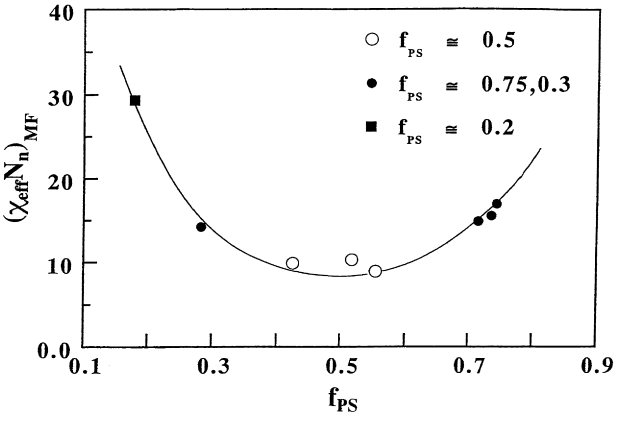

Fig. 10. $\chi_{eff}N_n$ at the crossover point $(\chi_{eff}N_n)_{MF}$ plotted as a function of f_{PS}.

and 0.19. The data points of WN were read from the figures in Ref. [22] (originally, D values were plotted against χ_{AB} values under the several conditions of various degrees of polymerization Z and polymer volume fraction ϕ_p) and we replotted the values of $D/Z^{0.5}$ against the $\chi_{AB}\phi_p Z$ ($= \chi_{eff}Z$) values. In the case of the LM prediction, D/R_g were plotted against the χN values. R_g and N stand for the radius of gyration and the total degree of polymerization of the

Table 6
Coefficients A and B, which determine temperature dependence of χ_{eff}, and crossover points $\chi_{eff,MF}$, $(\chi_{eff}N_n)_{MF}$ and $(\phi_p/T)_{MF}$ for a series of SI diblocks showing the cylindrical morphology

Sample code	f_{PS}	N_n	A[a]	B[a]	$\chi_{eff,MF}$[b]	$(\chi_{eff}N_n)_{MF}$[b]	$(\phi_p/T)_{MF} \times 10^3$ (K^{-1})[b]
HS-16	0.716	263	−0.0386	42.2	0.0566	14.89	2.256
HS-15	0.736	490	−0.012	29.6	0.032	15.54	1.484
HK-4	0.235	1383	0	13.1	0.0107	14.78	0.816
BSI-4	0.283	2220	0.0045	9.35	0.0068	15.07	0.24
BSI-9	0.641	2681	0.00606	8.26	0.0055	14.76	0.0375

[a] The values estimated from Figs. 10 and 11 in Ref. [18].
[b] The values estimated from Fig. 9.

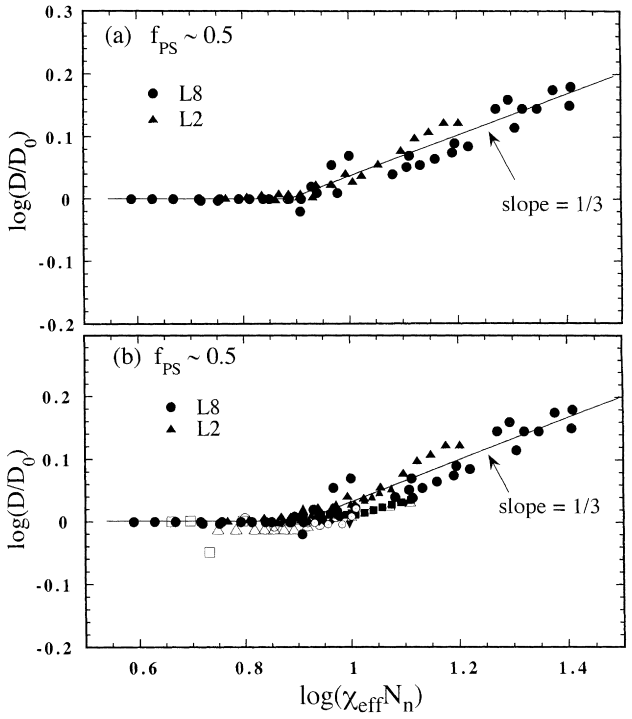

Fig. 11. Reduced wavelength D/D_0 plotted against the segregation power $\chi_{eff}N_n$ in double logarithmic scale for L-2 and L-8 (part a) and the comparison of the results for L-2 and L-8 (shown by filled circles and triangles) with those (shown by other open symbols) for the series of block copolymers with $f_{PS} \cong 0.5$ shown in Fig. 8a (part b). The data subjected to the non-equilibrium effects are omitted from these plots.

diblock copolymer, respectively. We replotted the value D/R_g divided by the value of the initial flat level at $\log(\chi_{eff}N) \sim 1.0$ against the χN values. The gap between WN and LM indicated by the arrow comes from the missing front factor ($= D_0/Z^{0.5}$). The experimental range of the segregation power covered is $\log(\chi_{eff}N) \leq 1.5$ for block copolymers with $f \cong 0.5$ and $\log(\chi_{eff}N) \leq 1.8$ for $f \cong 0.2$. The theoretical results for the block copolymers with $f = 0.5$ show a crossover in the scaling behavior of $D/D_0 \sim (\chi_{eff}N)^{\alpha}$ from the intermediate segregation regime with $\alpha = 1/3$ (WN) or $\alpha = 0.22$ (LM) to the strong segregation regime with $\alpha = 1/6$ (WN and LM) on increasing the segregation power $\chi_{eff}N$; the crossover $\chi_{eff}N$ depends on the theories. A similar crossover behavior was also predicted by Sones [24]. The theoretical results for the block copolymer with $f = 0.19$ also show the crossover from the intermediate segregation with $\alpha = 0.32$ to the strong segregation limit with $\alpha = 1/6$ [23]. The value α passes through a maximum value of 0.5 when the segregation power increases from the intermediate to the strong segregation.

Comparing the experimental results shown in Figs. 8, 11 and 12 with the theoretical results in Fig. 13 may indicate that $D \sim (\chi_{eff}N)^{1/3}$ at $(\chi_{eff}N) > (\chi_{eff}N)_{MF}$ is a result inherent in the weak-to-intermediate segregation, not yet approaching the theoretical strong segregation limit.

5. Conclusions

The characteristic length D of the dominant mode of the concentration fluctuations in both disordered and ordered states of the SI block copolymers having given f_{PS} and N_n was evaluated as a function of ϕ_p and T. The results obtained with a total of 20 block copolymers confirm the scaling law previously obtained with only the two block copolymers L-8 and L-2 [16,17]: (i) D is given by Eqs. (10) and (12); (ii) the crossover point, $(\phi_p/T)_{MF}$, is given by Eq. (13); and (iii) the proportionality constants of Eqs. (10), (12) and (13) depend on f_{PS}. The result given by Eq. (10) ($D_{order} \sim N_n^{2/3}$) is the well-known 2/3-power law. These experimental results were re-analyzed in terms of χ_{eff} measured previously [18] for the same copolymers as a function of ϕ_p and T (Eq. (4)). If the N_n-dependence of χ_{eff} given by Eq. (4) is true, then the results yielded the

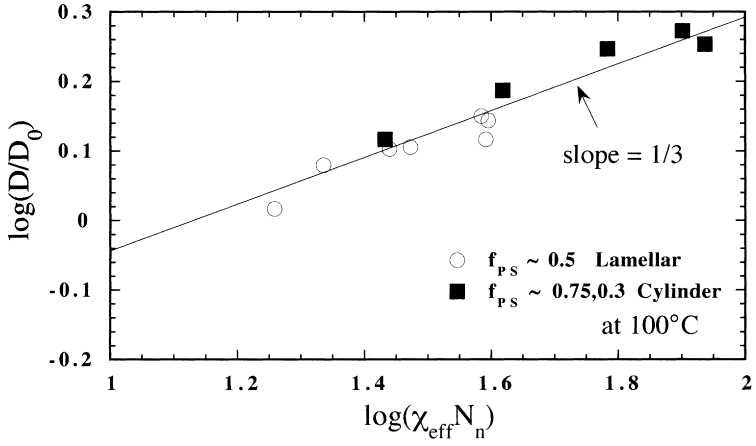

Fig. 12. Reduced wavelength D/D_0 plotted against the segregation power $\chi_{eff}N_n$ in double logarithmic scales for a series of lamella- and cylinder-forming block copolymers whose characteristics are shown in Tables 5 and 6, respectively. The data subjected to the non-equilibrium effects are omitted from these plots.

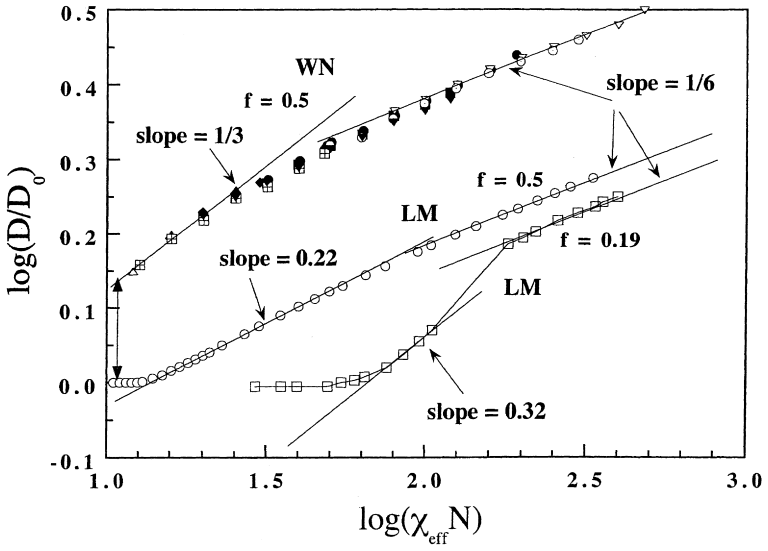

Fig. 13. Theoretically predicted reduced wavelength D/D_0 plotted against the segregation power $\chi_{eff}N$ in double logarithmic scale, WN and LM stand for Whitmore–Noolandi [22] and Lescanec–Muthukumar [23] predictions, respectively. N stands for total degree of polymerization (assumed to be monodisperse) of diblock copolymers.

scaling law given by Eqs. (18) and (19) over the molecular weight range covered in our experiment, implying that our systems studied here do not yet reach the theoretically predicted strong segregation limit. Thus the strange exponent of N_n in Eq. (13) can be still interpreted in the context of the mean-field approximation (Eq. (17)) together with the N_n-dependence of χ_{eff} (Eq. (4)). Further experimental studies, which invoke a systematic investigation of more precise temperature and concentration dependence, are desirable to find the ODT point $(\phi_p/T)_{ODT}$ for these block copolymers.

References

[1] Hashimoto T. In: Legge NR, Holden G, Schroeder HE, editors. Thermoplastic elastomers, 1st ed. Vienna: Hanser, 1987 (chap. 12).
[2] Hashimoto T. In: Legge NR, Holden G, Schroeder HE, editors. Thermoplastic elastomers, 2nd ed. Vienna: Hanser, 1996 (chap. 15A).
[3] Hasegawa H, Hashimoto T. In: Aggarwal SL, Russo S, editors. Comprehensive polymer science. New York: Pergamon Press, 1996 (2nd supplement; chap. 14; 497 p.
[4] Bates FS, Fredrickson GH. Annu Rev Phys Chem 1990;41:525.
[5] Brazovskii A. Sov Phys JETP 1975;41:85.
[6] Hashimoto T, Koga T, Koga T, Sakamoto N. In: Yonezawa F, Tsuji K, Kaji K, Doi M, Fujiwara T, editors. The physics of complex liquids. Singapore: World Scientific, 1998, 291 p.
[7] Leibler L. Macromolecules 1980;13:1602.
[8] Fredrickson GH, Helfand E. J Chem Phys 1987;87:697.
[9] Bates FS, Rosedale JH, Fredrickson GH. J Chem Phys 1990;92:6255.
[10] Stuhn B, Mutter R, Albrecht T. Europhys Lett 1992;18:427.
[11] Wolff T, Burger C, Ruland W. Macromolecules 1993;26:1707.
[12] Hashimoto T, Ogawa T, Han CD. J Phys Soc Jpn 1994;63:2206.
[13] Sakamoto N, Hashimoto T. Macromolecules 1995;28:6825.
[14] Sakamoto N, Hashimoto T, Kido R, Adachi K. Macromolecules 1996;29:8126.
[15] Floudas G, Pakula T, Fisher EW, Hadjichristidis N, Pispas S. Acta Polym 1994;45:176.
[16] Hashimoto T, Shibayama M, Kawai H. Macromolecules 1983;16:1093.
[17] Shibayama M, Hashimoto T, Hasegawa H, Kawai H. Macromolecules 1983;16:1427.
[18] Mori K, Okawara A, Hashimoto T. J Chem Phys 1996;104:7765.
[19] Helfand E. Macromolecules 1975;8:552.
[20] Hashimoto T, Mori K. Macromolecules 1990;23:5347.
[21] Helfand E, Tagami Y. J Chem Phys 1972;56:3592.
[22] Whitmore MD, Noolandi J. J Chem Phys 1990;94:2946.
[23] Lescanec RL, Muthukumar M. Macromolecules 1993;26:3908.
[24] Sones RA, Terentjev EM, Petschek RG. Macromolecules 1993;26:3344.
[25] Hashimoto T, Shibayama M, Nakamura N, Izumi A, Kawai H. J Macromol Sci Phys 1980;B17:389.
[26] Mori K, Hasegawa H, Hashimoto T. Polym J 1985;17:799.
[27] Mori K, Hasegawa H, Hashimoto T. Polymer 1990;31:2368.
[28] Helfand E, Wasserman ZR. Macromolecules 1976;9:879.
[29] Hashimoto T, Shibayama M, Kawai H. Macromolecules 1980;13:1237.
[30] Meier DJ. Prepr Polym Colloq Soc Polym Sci Jpn 1977:83.